

Osteological re-description of *Macrocnemus fuyuanensis* (Archosauromorpha, Tanystropheidae) from the Middle Triassic of China

Torsten M. SCHEYER^{1*}

WANG Wei^{2,3,4}

LI Chun^{3,4}

Feiko MIEDEMA^{1,5}

Stephan N. F. SPIEKMAN¹

(1 University of Zurich, Palaeontological Institute and Museum Zurich CH-8006, Switzerland

* Corresponding author: tscheyer@pim.uzh.ch)

(2 State Key Laboratory of Lithospheric Evolution, Institute of Geology and Geophysics, Chinese Academy of Sciences Beijing 100029, China)

(3 Key Laboratory of Vertebrate Evolution and Human Origins of Chinese Academy of Sciences, Institute of Vertebrate Paleontology and Paleoanthropology, Chinese Academy of Sciences Beijing 100044, China)

(4 CAS Center for Excellence in Life and Paleoenvironment Beijing 100044, China)

(5 Stuttgart State Museum of Natural History Stuttgart D-70191, Germany)

Abstract Over the past decades, an increasing number of reptiles have been described from the Middle Triassic of southern parts of China. Marine reptiles such as thalattosaurs, ichthyosaurs and sauropterygians dominated these paleofaunas and are known to have had a Tethys-wide distribution. Indeed, several species have been described from both the eastern and western margins of that ancient ocean. The last addition to this list was a less common terrestrial reptile, *Macrocnemus fuyuanensis*, first discovered in Yunnan Province. The species was also tentatively inferred to be represented by a single disarticulated specimen in the paleofauna from the World Heritage Site of Monte San Giorgio in southern Switzerland (as *Macrocnemus* aff. *fuyuanensis*). The initial referral was mainly based on limb proportions and ratios rather than on discrete osteological characters, partially due to a limited anatomical description of the holotype specimen of *M. fuyuanensis*. Here we provide a re-description of the anatomy of the complete skeleton of the holotype and compare it with the available referred specimens. Our re-analysis shows that the pectoral girdle of the holotype specimen is more complete than previously reported, revealing the shape of the interclavicle, which is only partially exposed in the only referred specimen from China but well-preserved in the specimen from Europe. The interclavicle of *M. fuyuanensis* can be distinguished from *M. bassanii* by its short and fusiform posterior process and anterior facing rod-like processes that extend from a common base enclosing a narrow V-shaped median notch, among other features, and is here inferred to be the most important bone for discriminating species of *Macrocnemus*, apart from the limb ratios. We further document in detail the cranial anatomy of the holotype, which is virtually identical to that of the crania of *M. bassanii*, and due

瑞士国家科学基金会(批准号: 205321_162775)、中国科学院战略性先导科技专项(B类)(编号: XDB26000000)和国家自然科学基金(批准号: 41772006)资助。

收稿日期: 2020-04-07

to its exquisite preservation and preparation, it adds important information on the palate, which was previously poorly known for *Macrocnemus*.

Key words Tethys, Triassic, Ladinian, Falang Formation, terrestrial reptile, archosauromorph, tanystropheid

Citation Scheyer T M, Wang W, Li C et al., 2020. Osteological re-description of *Macrocnemus fuyuanensis* (Archosauromorpha, Tanystropheidae) from the Middle Triassic of China. *Vertebrata Palasiatica*, 58(3): 169–187

1 Introduction

Recently, Jaquier et al. (2017) described a new specimen (PIMUZ T 1559) of *Macrocnemus* from the Middle Triassic of Switzerland. The authors found the proportions of the forelimb bones in this specimen were in congruence with specimens of the species *Macrocnemus fuyuanensis* from China (Li et al., 2007) but differed from other European specimens of *Macrocnemus*. As such, the new European specimen was tentatively assigned to *Macrocnemus* aff. *fuyuanensis*. In addition, it was pointed out by Jaquier et al. (2017) that some obvious morphological differences exist between the interclavicle of PIMUZ T 1559 and that of the other Swiss specimens of *M. bassanii*, in which the interclavicle is preserved. Jaquier et al. (2017) concluded that the interclavicle could thus reveal potentially diagnostic characters for *Macrocnemus* species identification, once interclavicles were better identified and described in the Chinese specimens.

In the original description of *M. fuyuanensis*, the pectoral girdle was not treated in much detail and the presence of an interclavicle was not mentioned. In the description of the only referred specimen from China, GMPKU-P-3001, Jiang et al. (2011) noted the presence of the interclavicle, which was mostly hidden underneath other appendicular and axial elements, revealing only a portion of its anterior margin. Jiang et al. (2011) further noted that the anterior margin appears damaged, but the nature of the damage was not clear from the description or corresponding figure. Jaquier et al. (2017) therefore indicated that neither of the two known Chinese specimens shows a well-exposed interclavicle. A close examination of the pectoral girdle of the holotype IVPP V 15001, however, reveals that an interclavicle is indeed present and well exposed, although it is partially broken. We here report on the osteology of this bone and that of the other pectoral girdle elements and reveal its importance in differentiating *M. fuyuanensis* and *M. bassanii*.

Additionally, we here present a re-analysis of the anatomy of the holotype of *M. fuyuanensis* and compare it with the available referred specimens GMPKU-P-3001 and PIMUZ T 1559. We infer that such documentation will help greatly in future taxonomic identification of *Macrocnemus* material and our general understanding of the anatomy of this genus.

2 Material and methods

As indicated by Li et al. (2007) and Jiang et al. (2011), both described Chinese specimens of *Macrocnemus fuyuanensis* originate from one locality in the Falang Formation (latest Ladinian-earliest Carnian) in Fuyuan, Yunnan Province, southwestern China. The so far only known European specimen of *Macrocnemus* aff. *fuyuanensis*, described by Jaquier et al. (2017), was found in the upper Besano Formation (late Anisian) at locality Mirigioli/point 902 near Meride, Monte San Giorgio, Canton Ticino, Switzerland. For the present study, the holotype and referred specimen of *M. fuyuanensis* and the Swiss specimen were compared and checked closely for the presence and shape of the interclavicle. For measurements of the interclavicles of all three specimens taken with digital calipers, see Table 1. Additional measurements of limb bones and vertebrae have been published in previous publications (see tables in Li et al., 2007; Jiang et al., 2011; Jaquier et al., 2017). Pictures of specimens were taken with a CANON digital SLR camera EOS 750D, and assembled and processed in Adobe CC (Photoshop and Illustrator).

Table 1 Length measurements of the interclavicle of *Macrocnemus fuyuanensis* (mm)

	IVPP V 15001	GMPKU-G-3001	PIMUZ T 1559
Maximum width (as preserved)	40.44	40.01	31.50
Maximum width (estimated)*	ca. 55	ca. 48	ca. 35
Maximum length	68.69		43.35
Thinnest shaft diameter at constriction	4.89		2.48
Thickened shaft diameter	7.70		3.68
Length of caudal process (from constriction to tip of process)	35.64		21.65
Maximum width of anterior tips of V-shaped median notch	8.19		3.80
Ratio length of caudal process / maximum length	0.52		0.49

* Estimated maximum widths are based on duplication of single wing-like extension measurements to the mid-line (referred specimens), or based on outline comparison (in case of the holotype).

Institutional abbreviations GMPKU, Geological Museum of Peking University, Beijing, China; IVPP, Institute for Vertebrate Paleontology and Paleoanthropology, Chinese Academy of Sciences, Beijing, China; PIMUZ, Paleontological Institute and Museum, University of Zurich, Switzerland.

3 Systematic paleontology

Archosauromorpha Huene, 1946

Tanystropheidae Camp, 1945

Macrocnemus Nopcsa, 1930

Macrocnemus fuyuanensis Li et al., 2007

(Fig. 1)

Specimens examined IVPP V 15001 (holotype, adult); GMPKU-P-3001 (referred specimen, adult); PIMUZ T 1559 (referred specimen, subadult).

Locality and horizon Eastern Tethyan province: IVPP V 15001, GMPKU-P-3001;

Fuyuan, Yunnan Province, southwestern China; Zhuganpo Member, Falang Formation (Ladinian, Middle Triassic; note that for GMPKU-P-3001, an age range of latest Ladinian-earliest Carnian was provided by Jiang et al., 2011). Western Tethyan province: PIMUZ T 1559; Meride, Ticino, Switzerland; upper Besano Formation (late Anisian, Middle Triassic).

Emended diagnosis Species of *Macrocnemus* up to 120 cm body length in total; humerus considerably longer than radius (~20%); interclavicle developing wide wing-like lateral processes with pointed tips, with smooth ventral bone surface, with anterior rod-like processes extending from a common base and enclosing a narrow V-shaped median notch; interclavicle caudal process short, constituting about half of the total length of the bone, fusiform shape, being expanded in mid-shaft region and having a rounded posterior tip.

4 Re-description

IVPP V 15001 (Fig. 1) is still the largest *Macrocnemus* specimen known to date (Li et al., 2007; Jaquier et al., 2017). A large part of the specimen is still articulated, although some components such as the cranium, lower jaw, girdles, and limbs have shifted out of position in respect to the mostly articulated vertebral column. In the cranium, the anterior palatal elements and the cranial roof- and circumorbital bones have disarticulated, whereas the posterior bones of the braincase region are still mostly in contact and visible in ventral view. The largely articulated rami of the lower jaw are seen in an angled ventral view. The cervicals and anterior trunk vertebrae from the axis to dorsal vertebra 6 are visible in right lateral view, dorsal vertebra 7 to caudal vertebra 16 are in dorsal view, caudal vertebra 17 to 24 in right lateral view, and finally, caudal vertebra 25 to 44 are visible in left lateral view. Though dislocated, most elements of the pectoral girdle and the right pelvic bones remained in close association to each other. In the limbs, the bones of the right fore- and hind limb are mostly articulated and seen in dorsal and ventral views, respectively.

Cranium In the cranium, many bones of the braincase, including the exoccipitals, opisthotics, basioccipital, parabasisphenoid, and supraoccipital could be identified (Fig. 2). The supraoccipital, basioccipital and parabasisphenoid are exposed in slightly angled ventral view. Of the palate, both pterygoids and the right epipterygoid remained in close contact with the braincase elements, whereas the anterior elements of the palate, the palatines and the vomers, have been farther displaced. The vomers are rotated about 180 degrees and lie now posterior to the occipitals. Similarly, the maxillae and premaxillae (the left one is mostly hidden by the right one) are directed now in posteromedial and posterior direction respectively and tooth counts are obscured due to overlap by other bones. Two elongated rod-like bones (ca. 35 mm in length) are here identified as the ceratobranchials I of the hyoid apparatus, which have also been described for PIMUZ T 1559 (Jaquier et al., 2017).

Of the cranial roof, only the left frontal is visible in ventral view, exposing a thickened orbital rim and the posterolateral process. The parietals are likely completely covered by

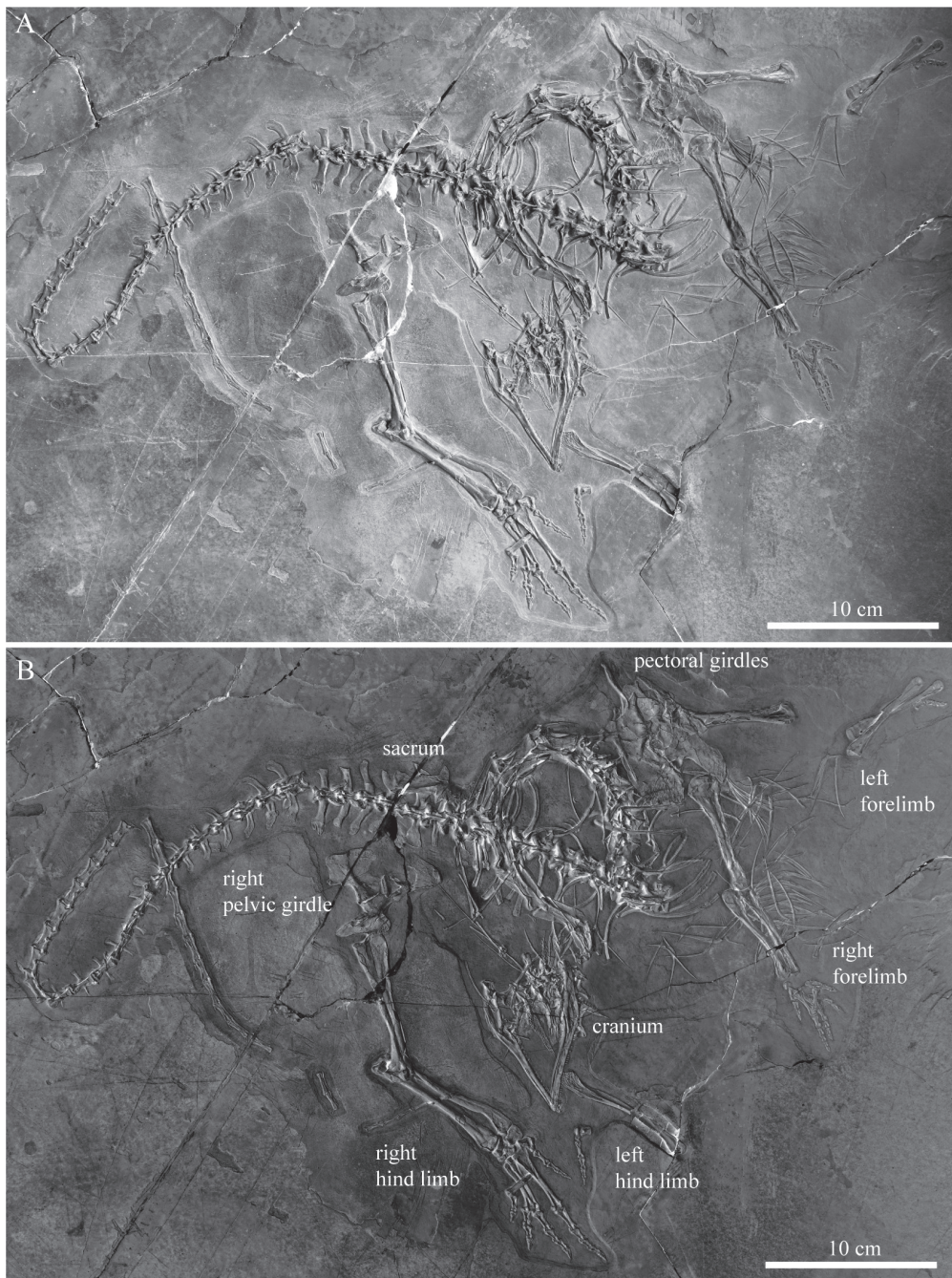


Fig. 1 Overview image (A) and inverted color image enhancing bone identification (B) of IVPP V 15001, holotype of *Macrocnemus fuyuanensis*

other cranial bones, except a potential curved posterolateral process that is exposed at the posterior margin of the left parietal (noted as an asterisk in Fig. 2). A similar process was figured and described for the parietal in GMPKU-P-3001 (Jiang et al., 2011; Jaquier et al.,

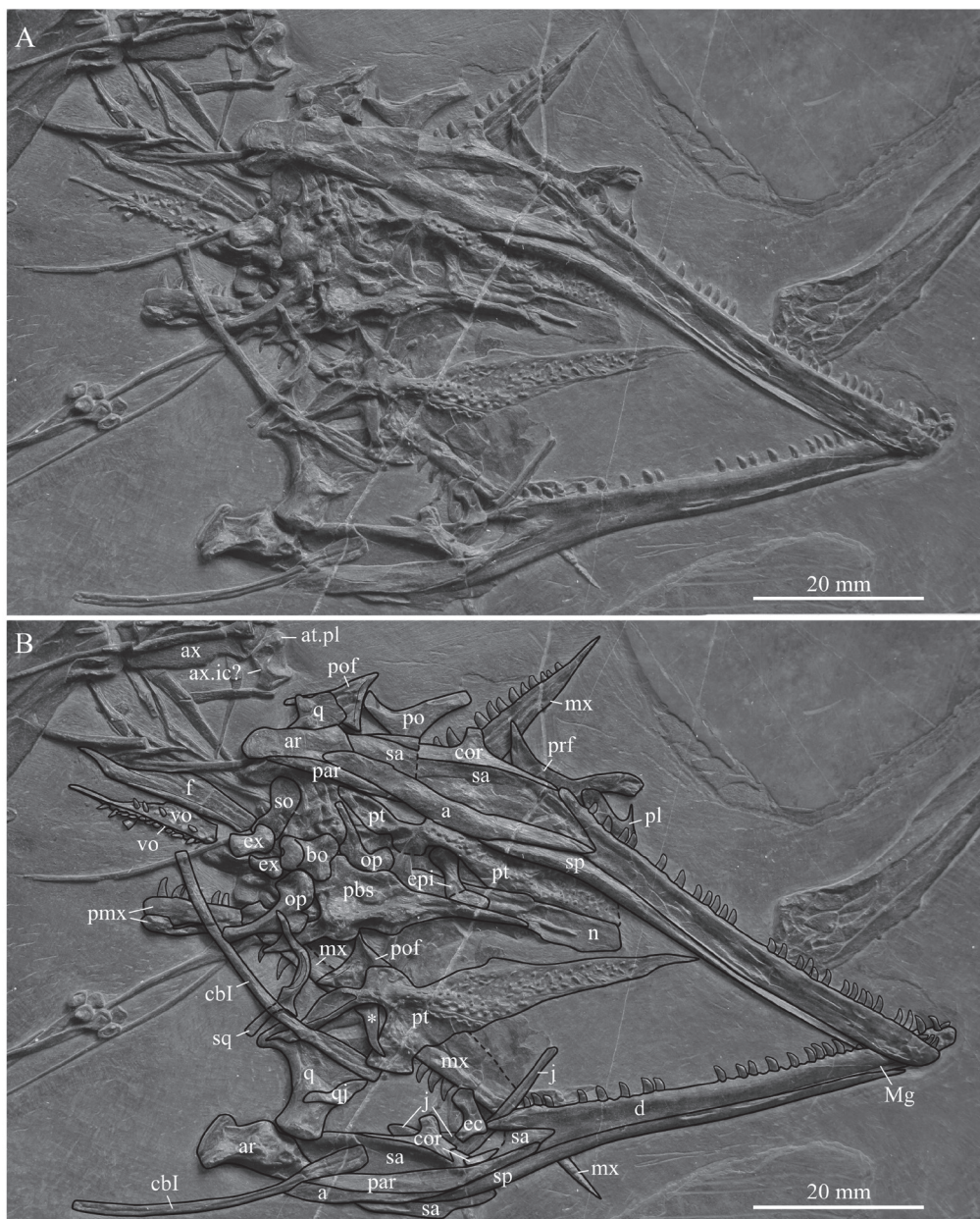


Fig. 2 Close-up view (A) and interpretative drawing (B) of the cranium and lower jaw of IVPP V 15001, holotype of *Macrocnemus fuyuanensis*

Abbreviations: a. angular; ar. articular; at.pl. atlantal pleurocentrum; ax. axis; ax.ic. axis intercentrum; bo. basioccipital; cbl. ceratobranchial I; cor. coracoid; d. dentary; ec. ectopterygoid; epi. epipterygoid; ex. exoccipital; f. frontal; j. jugal; Mg. Meckelian groove; mx. maxilla; n. nasal; op. opisthotic; par. prearticular; pbs. parabasisphenoid; pl. palatine; pmx. premaxilla; po. postorbital; pof. postfrontal; prf. prefrontal; pt. pterygoid; q. quadrate; qj. quadratojugal; sa. surangular; so. supraoccipital; sp. splenial; sq. squamosal; vo. vomer; * posterior process of parietal

2017). The left pterygoid is complete and exposed in ventral view, revealing several rows of either small teeth or small alveoli on the tapering palatal ramus. The tips of the pterygoids converge towards the sagittal plane, delimiting the interpterygoid vacuity anteriorly. Anterior to the large field of teeth (individual rows are difficult to discern), there is a small lunate facet laterally for either the palatines or the vomers (Fig. 3A). Further posteriorly, the medial bone margin is first weakly concave and then more strongly concave from about mid-length of the pterygoid, followed by a broad and posteromedially extending process. This process articulates with the basiptyergoid process of the parabasisphenoid (presumably separated by a cartilaginous joint acting as buffer between the bones). This is followed posteriorly by the slender and tapering quadrate ramus. Laterally, the pterygoid has a broad and posterolaterally extending transverse flange-like process. It carries an anteromedial-posterolateral trending row of teeth on the posterior edge of the flange (Figs. 2, 3; corresponding to row T1 as identified by Welman, 1998). The articulation facet for the ectopterygoid is not well defined, but appears to lie somewhat anterior to the transverse process along the lateral bone margin of the tapering palatal ramus. Only one anterior half of a palatine is visible underneath the posterior tooth row of the right dentary showing the posterior margin of the internal naris (Fig. 2). Of the left jugal, only the anterior and dorsal processes are visible, since this element is otherwise covered by the left ramus of the lower jaw. The other circumorbital bones such as the prefrontal, postorbital or postfrontal are also only partially exposed. The small bone overlying the left jugal was identified as an ectopterygoid, possibly the left one. The posterior flattened part of the nasal was identified between the pterygoids, indicating that the rod-like anterior process of the nasal is hidden by the braincase elements. The exposed flattened part of the purported nasal is of the same shape and carries a ridge, as in the nasal described by Jaquier et al. (2017:fig. 3K) for PIMUZ T 1559. The left quadrate is more exposed than the right one, and in close association with the left articular, a small and curved bone interpreted herein as a quadratojugal, and the squamosal. The latter carries four distinct processes and is rotated so that the head of the quadrate lost its articulation with the quadrate facet (visible on the bone as a concavity).

Lower jaw The two rami of the lower jaw (Fig. 2) are still in contact in the symphyseal region, with the right one being visible in lateral view and the left one in medial view. Both rami are to a large degree still in articulation, but in the left ramus the posterior portion has been angled ventrally and a small portion of the medial side of the angular got exposed ventral to the articular. In the right ramus, the posterior portion is displaced dorsally, so that the angular, surangular and coronoid show a break in their anterior portions. The dentary is the only tooth-bearing bone in the lower jaw. The right dentary has 28 recurved teeth still embedded, the left one 21. Given the number of alveolar spaces on the dentaries, the maximum number of teeth would have been 40–42, not 45–50 as Li et al. (2007) previously estimated. This is in congruence with the other large specimen, GMPKU-P-3001, whereas the smaller PIMUZ T 1559 seems to have carried fewer teeth (<30). The splenial extends along the lower

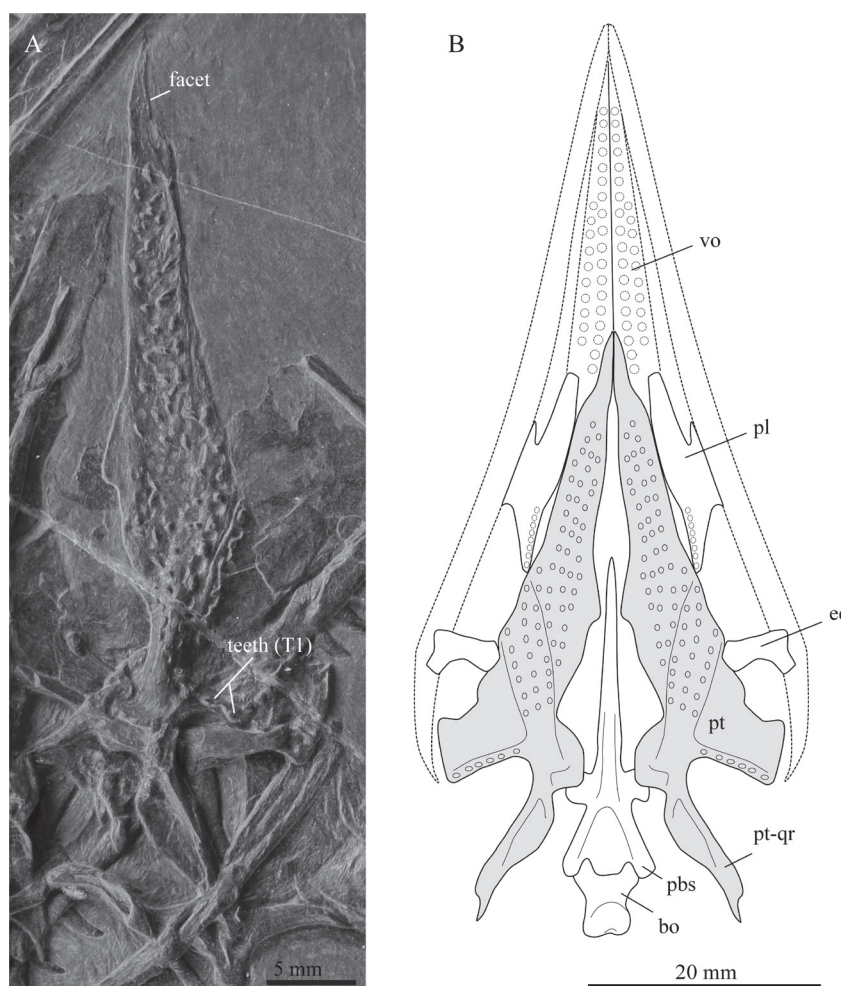


Fig. 3 Image of left pterygoid (A) of IVPP V 15001, holotype of *Macrocnemus fuyuanensis* and reconstructive sketch (B) of the pterygoids and surrounding bones

The basioccipital, the pterygoid (in grey), and the ectopterygoid were taken from IVPP V 15001 and are to scale (the latter two were also mirrored for completion). The parabasisphenoid and the palatine were taken from PIMUZ T 1559 and rescaled (the latter also mirrored as well). Stippled lines indicate the outlines of the upper jawbones (premaxilla, maxilla and jugal) and the vomers. The outline and dentition of the vomer is only incompletely preserved in IVPP V 15001. Note that the posteromedial gap between pterygoid and tooth-bearing margin of the palatine in the sketch might be a preservational artefact

Abbreviation: pt-qr. quadrat ramus of pterygoid; other abbreviations see Fig. 2

margin of the dentary but does not reach the symphysis, thus the Meckelian groove is exposed anteriorly for a short distance on the medial side of the dentary. The surangular is capped by the coronoid, which carries a distinct rectangular process situated about half mid-length of the bone. The angular and the prearticular are both weakly bow-shaped. The angular is completely exposed laterally in the right ramus, articulating anteriorly with the dentary, dorsally with the surangular, posteriorly with the articular, anteroventrally with the splenial and posteroventrally with the prearticular. The posterolateral part of the prearticular is exposed in the right ramus

and the complete mid and anterior portion of the medial side in the left ramus. On both sides the articular shows a short retroarticular process and remains in articulation with its respective quadrate.

Vertebral column We confirm the presence of eight cervicals. Of the atlas complex, only the pleurocentrum is identified, which remains in contact with the anterior articular facet of the axis. At the anteroventral border of the axis, a roughly dumbbell-shaped bone is tentatively identified as the axis intercentrum. The axis and following cervical vertebrae are well exposed and remain in articulation with the following six anterior dorsal vertebrae (Fig. 4A). Anterolaterally, the axis shows an oval shaped articulation facet, the prezygapophysis, which would have articulated with the atlantal neural arch. The axial neural spine is slightly declining in height anteroposteriorly. The posterior border of the axial neural spine is concave to accommodate the anterior process of the spine of the following 3rd cervical. The postzygapophyses also extend beyond the posterior margin of the axis centrum, to accommodate the robust prezygapophyses of the 3rd cervical. Cervicals 3 to 8 have flattened and dorsally expanded neural spines; similar spine shapes have been described also for other Late Triassic tanystropheids (Pritchard et al., 2015). Their postzygapophyses are well-developed and have a slight bulbous expansion on their dorsal surface, the epipophysis, which represents an attachment site for neck musculature. Although distinct, these epipophyses are less pronounced, and do not extend as far posteriorly, as in *Tanystropheus* (Spiekman and Scheyer, 2019). The cervical ribs are all double-headed and bear a short and stout anterior process. As noted by Li et al. (2007), the total length of the cervical ribs is difficult to assess in the specimen. Through comparison with PIMUZ T 1559 it is apparent that most of them are broken and that the thin elongated rod-like and tapering bones represent the distal portions of the cervical ribs. These cervical ribs could span up to three adjacent cervical centra and thus are comparable in relative elongation to the cervicals of *Tanystropheus* and *Dinocephalosaurus* (Rieppel et al., 2008; Spiekman and Scheyer, 2019). The last cervical only has a short cervical rib, which is still in articulation.

There are 17 dorsal vertebrae, not 17–18 as previously stated (Li et al., 2007). Those anterior dorsals that are exposed in lateral view show the strong diapophysis of the neural arch and the parapophysis for the double-headed dorsal ribs. Towards posterior, the diapophyses and parapophyses become confluent and towards the sacrum, there is just a simple single attachment facet for a single-headed rib. The ribs curve gently, lack flange-like protrusions or uncinate processes and expand slightly distally. The posterior dorsal vertebrae in dorsal view show the overlapping zygapophyses and low neural spines. The two sacrals are not well exposed (Fig. 4A), with the left rib of the first sacral being hidden underneath the partially damaged left ilium and the second sacral being strongly affected by a crack through most of the bone. Li et al. (2007) noted the bifurcation of the rib of the second sacral and the overlap of the posterior process of the first sacral with the anterior process of the second sacral laterally. The anterior caudals show caudal ribs that are angled posteriorly. Some of the ribs of the proximal

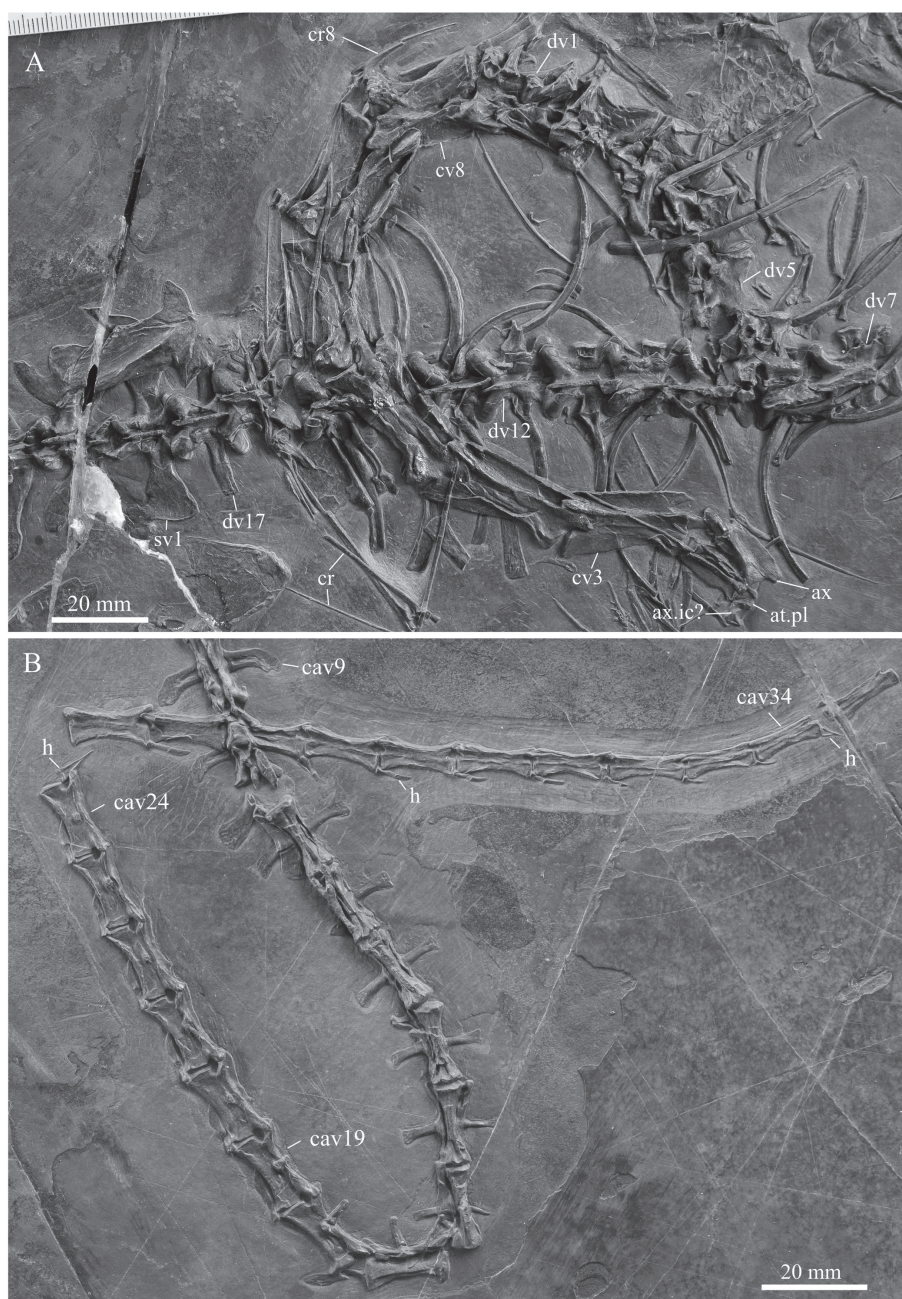


Fig. 4 Close-ups of the cervico-dorsal (A) and major part of the caudal (B) vertebral column of IVPP V 15001, holotype of *Macrocnemus fuyuanensis*

Abbreviations: cav. caudal vertebra; cr. cervical rib; cv. cervical vertebra; dv. dorsal vertebra; h. hemal arch; sv. sacral vertebra; other abbreviations see Fig. 2

caudal vertebrae also show a distal anteroposterior broadening (e.g., in caudal vertebra 3), that are capped by one or two lappet-like protrusions (presumably osseous, but they could also be calcified cartilage). Large caudal ribs are preserved only until caudal vertebra 19

(Fig. 1), whereas towards posterior, these become increasingly smaller and knob-like, and can be seen on the lateral sides only up to caudal centra 24 (Fig. 4B). Hemal arches articulate posteroventrally with the caudal vertebral centra. The hemal arches are Y-shaped with a proximal connection at least until caudal centra 24, and posteriorly—as is visible in caudal vertebrae 34 and 37—the proximal connection is lost.

Pectoral girdle Of the pectoral girdle, the interclavicle, the left clavicle, and both scapulae and coracoids could be unambiguously identified in IVPP V 15001 (Fig. 5). A rod-like element that is partially hidden by the interclavicle is interpreted as a rib. Furthermore, the interclavicle, preserved in dorsal view, is covering the medial portion of the left clavicle, the anterior portion of the right coracoid, and the left coracoid almost completely. All girdle elements have shifted out of their natural position and are over- and underlain by other axial and appendicular bones, but the left clavicle has shifted only slightly from the articulation with the interclavicle and the right scapula still remains in articulation with the right coracoid in medial view. The articular facet of the left scapula and that of the left coracoid is hidden beneath the interclavicle. In the following, the girdle elements of the holotype specimen of *M. fuyuanensis* will be briefly described individually.

The scapula is a large flat element with an extended posterodorsal blade and a straight ventral articulation with the coracoid. The anterior and anterodorsal margins of the scapula are not well preserved in both the left and right bone due to compaction and fracturing. The scapular portion of the glenoid facet is not visible. The coracoid is oval in shape and the articulation for the scapula is slightly offset. The lateral surface is slightly convex, with the anterior portion being slightly longer than the posterior portion. Close to the articular facet for the scapula, a kidney-shaped coracoid foramen is visible in the right coracoid. The coracoid portion of the glenoid facet is also not visible. Anterior to the connection between the right scapula and coracoid, a large anteriorly open fenestra is present between the two elements.

The left clavicle is preserved in anterodorsal view. It is a thin curved bone, with a slight torsion that separates a medial flattened part with an articular groove and a dorsal, also somewhat extended, part ending in a blunt stub laterally. The interclavicle is T-shaped with laterally expanded wing-like processes and a prominent fusiform caudal process. The lateral-most tips of the wing-like expansions are not preserved. Medially the interclavicle shows a narrow anterior outgrowth of bone extending into a V-shaped median notch. Lateral to the notch the anterior margins of the interclavicle are slightly concave. Posteriorly, the wing-like lateral expansions grade into the caudal fusiform process, a transition that is marked by a clear constriction of the bone. The fusiform caudal process then expands at the mid-shaft region and terminates in a blunt posterior tip. Due to the preservation of the interclavicle in dorsal view, the anterior articular facets for the clavicles cannot be seen, but they are represented by a slight thickening of the bone.

Forelimb Of the left forelimb, the isolated humerus, articulated zeugopodial elements, and the fifth digit are preserved. The right forelimb is more complete (Fig. 6), showing a

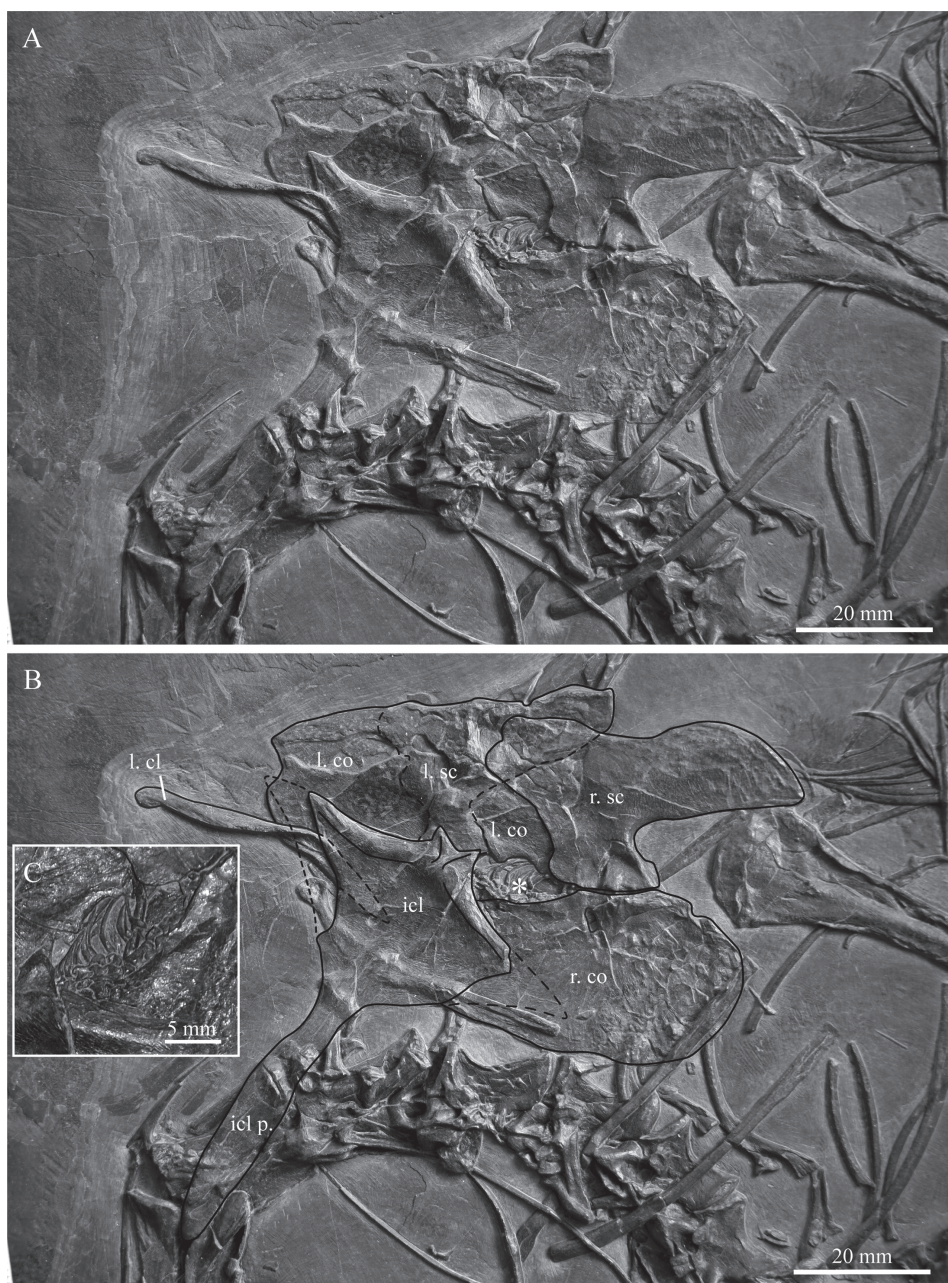


Fig. 5 Close-up view (A) and interpretative drawing (B) of the pectoral girdle bones in IVPP V 15001, holotype of *Macrocnemus fuyuanensis*

Small skeletal remains (close-up in C), possibly from a small *Keichousaurus* sp.,

are indicated by an asterisk (*) in the embayment between scapula and coracoid

The lateral tips of the wing-like extensions of the interclavicle are tentatively indicated based on the outline of the bone in the European specimen PIMUZ T 1559

Abbreviations: cl. clavicle; co. coracoid; icl. interclavicle; l. left; p. process; r. right; sc. scapula

humerus with a convex proximal head that appears to be greatly expanded compared to the distal end, which is also distinctly convex in dorsal view. This, however, is likely due to the preservation and particular orientation of the bone in the sediment as a) the distal condyles in the left humerus are less constricted and b) other specimens of *Macrocnemus* show much broader distal condyles as well (Peyer, 1937; Jaquier et al., 2017). The proximal head of the radius is flat, whereas the ulna has a large proximal expansion but a smaller articular facet for the humerus and a low acromion process. Distally, both the radius and ulna show convex condyles, with the ulnar condyle being slightly more expanded. There are six carpal elements in the right hand (Fig. 6B), followed by five digits (phalangeal count 2-3-4-5-3). Rieppel (1989) mentioned and illustrated the manus with five carpals in specimen PIMUZ T 2474 of *M. bassanii*. Following that study, the largest of the carpal bones likely represents the intermedium, the bone proximal to digit 1 the distal carpal 1, the bone proximal to digits 3 and 4 distal carpal 4. The other carpal elements are too scattered to be identified confidently.

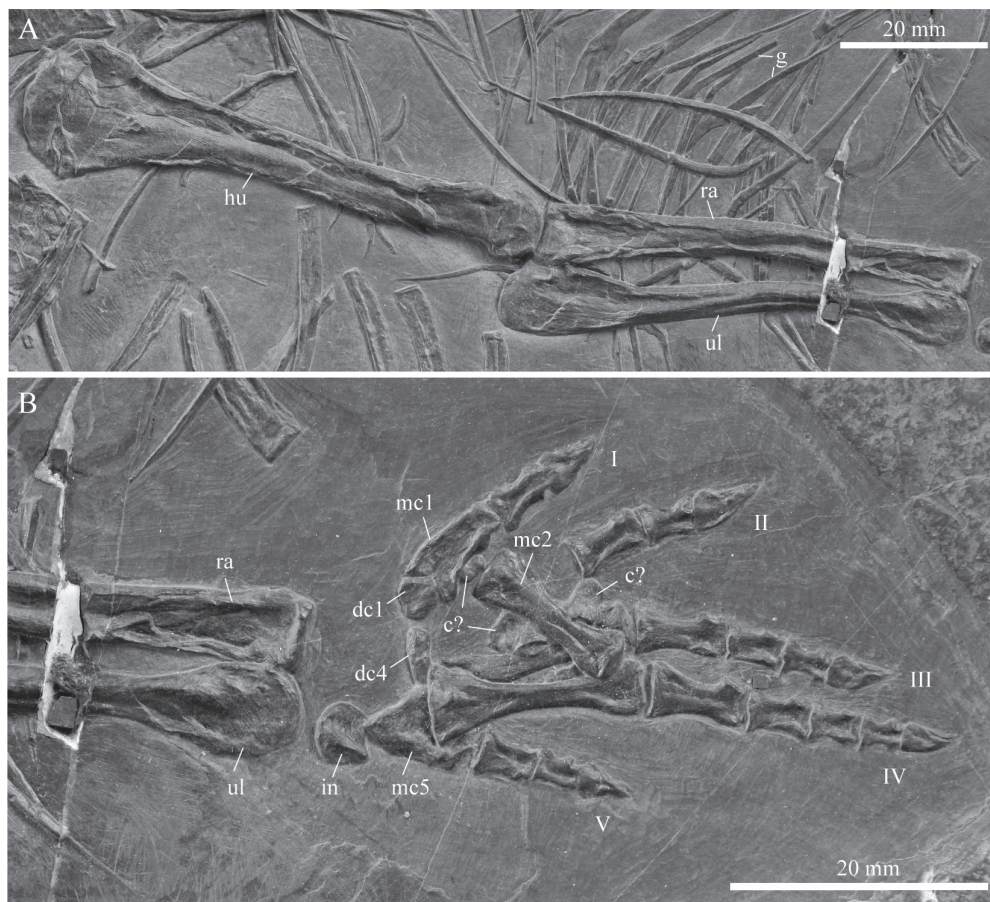


Fig. 6 Close-up of the stylo- and zeugopodial (A) and autopodial (B) elements of the right forelimb of IVPP V 15001, holotype of *Macrocnemus fuyuanensis*

Abbreviations: c. carpal; dc. distal carpal; g. gastralia; hu. humerus; I-V. indicate the digits in the manus; in. intermedium; mc. metacarpal; ra. radius; ul. ulna

Pelvic girdle Of the left pelvic girdle, the ilium overlies the sacrum, whereas what looks to be the left pubis is barely visible among the posterior trunk vertebrae. The right pelvic girdle is well exposed in medial view, showing the tripartite arrangement with the dorsal ilium, the posteroventral ischium and the anteroventral pubis still in articulation (Fig. 7). All three elements participate in the formation of the acetabulum accommodating the femoral head. The shaft region of the pubis and the distal margin of the ischium are slightly damaged, but the shape of both bones is still well discernible. IVPP V 15001 and PIMUZ T 1559 both show a smooth preacetabular margin of the ilium without a distinct process or tuber (not discernable in GMPKU-G-3001). Such a distinct process appears to be variably present in specimens of *M. bassanii* and other tanystropheids (Pritchard et al., 2015).

Hind limb The left hind limb is represented only by the femur and the fifth digit, whereas the right hind limb is completely preserved and visible in ventral view (Fig. 8). Li et al. (2007) mentioned six ossified tarsals in the hind limb, without providing additional details as to their shape or identification, but stated the phalangeal count of the pes to be 2-3-4-5-4. As in *M. bassanii* (Rieppel, 1989), the tarsus of IVPP V 15001, preserved in plantar view, shows a large blocky calcaneum between the fibula and the fifth digit, in articulation with an elongated astragalus lying distal to the tibia (Fig. 8B). Both proximal tarsal elements enclose a foramen for the perforating artery. Following Rieppel (1989), the remaining tarsals are interpreted

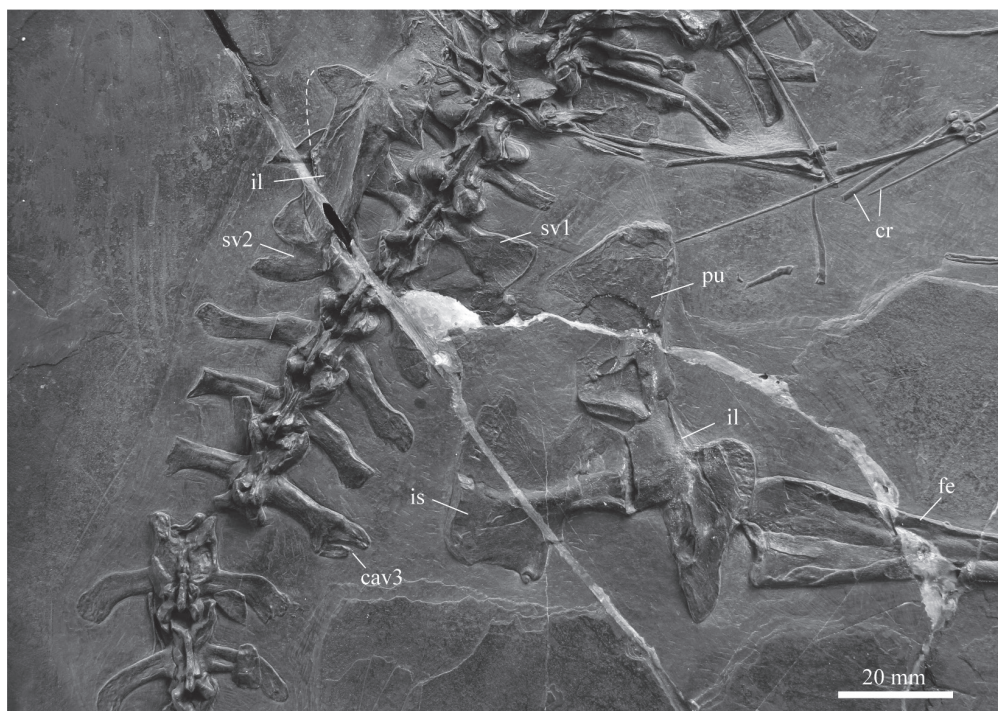


Fig. 7 Close-up of the sacral region and pelvic girdle in the holotype specimen IVPP V 15001 of *Macrocnemus fuyuanensis*
Abbreviations: cav. caudal vertebra; cr. cervical rib; fe. femur; il. ilium; is. ischium;
pu. pubis; sv. sacral vertebra

as the centrale and distal tarsals 1, 3 and 4, with the last of these being the largest. The fifth metatarsal is hooked and much shorter compared to the other metatarsals, which are straight and elongate (getting larger and more robust from digit 1 to digit 4).

Gastral apparatus Most gastralia can be found in the anterior trunk region, close to the right forelimb (Fig. 6A). They show a staggered composition of paired, elongated, laterally and medially tapering elements. Some elements appear bifurcated, which might be the result of medial fusion of gastral elements.

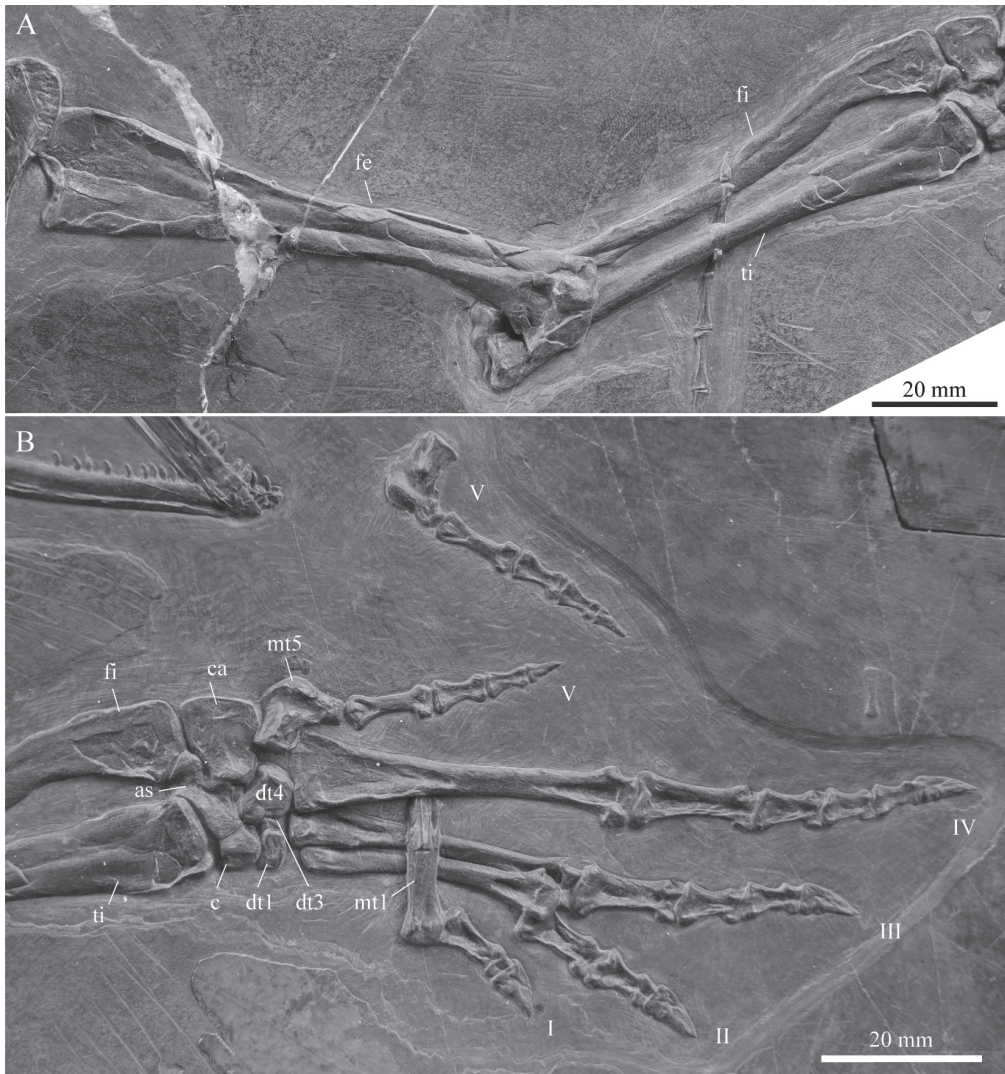


Fig. 8 Close-up of the stylo- and zeugopodial (A) and autopodial (B) elements of the right hind limb in IVPP V 15001, holotype of *Macrocnemus fuyuanensis*

Note the tip of the tail overlying the zeugopodial bones in A and the isolated fifth digit of the left hind limb in B

Abbreviations: as. astragalus; c. centrale; ca. calcaneum; dt. distal tarsal; fe. femur; fi. fibula;

I-V. indicate the digits in the pes; mt. metatarsal; ti. tibia

Additional bones on the slab of IVPP V 15001 It is noteworthy that within the fenestra formed between the right scapula and coracoid, the remains of a partial skeleton, possibly of a *Keichousaurus* sp., are visible (Fig. 5B, C). This is indicated by the presence of a string of articulated vertebrae (eight or nine, as indicated by neural arches seen in dorsal view) and only slightly dislocated ribs. Although the small saurian remains thus appear to lie within the anterior body cavity of IVPP V 15001, the disarticulation of the *M. fuyuanensis* specimen, combined with the fine preservation and articulated state of the partial skeleton, argue against it being stomach content. Additional bones that do not belong to the holotype of *M. fuyuanensis* include an isolated phalanx (in close proximity to the fourth digit of the right pes) and an isolated digit including an ungual phalanx (close to the right hand), which appear to belong to smaller indeterminate reptile.

5 Discussion and conclusions

The pattern of cranial and mandibular disarticulation indicates that the head was embedded ventrally in the sediment prior to diagenesis and fossilization. As such, braincase elements remained rather stable after the head separated from the cervical column and it is mostly the anterior cranial elements (including the vomers and palatines), as well as the cranial roof and circumorbital bones, that experienced most postmortem displacement. Of the postcranium, the right appendicular elements also remained in closer contact compared to the left side. The vertebral column, on the other hand, experienced only some separation of the neck and anterior dorsal (thoracic) region from the posterior trunk and a few minor breaks in the tail region.

Comparison of the cranium and lower jaw of the holotype with the referred specimens revealed a few ontogenetic changes, such as the increasing number of marginal teeth in the dentary and maxilla, similar to changes observable between smaller and larger specimens of *M. bassanii* (e.g., Peyer, 1937; Kuhn-Schnyder, 1962). Apart from this, the bones are virtually identical in shape between *M. fuyuanensis* and *M. bassanii* (the cranium and mandible of *M. obristi* Fraser and Furrer, 2013 are not known) and thus currently provide no characters for species separation (a revision of the cranial anatomy of *M. bassanii* is currently in progress elsewhere). The complete and well-preserved pterygoid of IVPP V 15001, together with several adjacent bones in V 15001 and PIMUZ T 1559, allow the partial reconstruction of the palate of *M. fuyuanensis* in ventral view (Fig. 3B).

The postcranial bones of both *M. fuyuanensis* and *M. bassanii* are very similar to each other as well, with the exception of the interclavicle in the pectoral girdle. The description of the pectoral girdle of the holotype specimen IVPP V 15001 of *M. fuyuanensis* is thus important for species recognition. Although the holotype is distinctly larger than the smaller European specimen PIMUZ T 1559 from Switzerland, the identifiable shape of the bones is mostly congruent. The identification of the interclavicle in V 15001 allows for the reassessment of the

previous assignment of PIMUZ T 1559 to *M. aff. fuyuanensis*, because several of the proposed diagnostic features of the interclavicle of that specimen are clearly recognizable in V 15001 as well. These are the narrow outgrowth with V-shaped anterior notch on the anterior end, the slightly concave anterior margins laterally to the notch, a clear constriction between the wing-shaped lateral expansions and the caudal process, and a short fusiform caudal process with an expanded mid-shaft section and a blunt posterior tip that constitutes only about half of the maximum length of the bone (Table 1). Unfortunately, due to preservation, the lateral shape of the wing-like expansions or the potential presence of circular emarginations close to the tips of the wings as described in PIMUZ T 1559 cannot be assessed in the holotype (for a detailed comparison with the interclavicle of *M. bassanii*, see Jaquier et al., 2017).

In the referred specimen GMPKU-G-3001, the partial anterior portion of the T-shaped interclavicle is visible in dorsal view. The complete anterior left wing-like expansion is exposed so that taking width measurements of that side is possible. Although noted as having a damaged anterior margin by Jiang et al. (2011), the bone nevertheless also reveals a narrow anterior outgrowth forming a V-shaped instead of a broad u-shaped notch. The left wing-like expansion is furthermore quite narrow, more similar to the condition seen in PIMUZ T 1559 than in specimens PIMUZ T 4355 and PIMUZ T 2475 of *M. bassanii* (see Jaquier et al., 2017:fig. 7).

Finally, the general shape of the pectoral bones in the holotype (IVPP V 15001) corroborates the configuration of the pectoral girdle as proposed by Jaquier et al. (2017) in that the scapulocoracoid articulation shows a large fenestra between the elements instead of a close contact. The clavicles articulate with the interclavicle with their medial expanded portion, whereas their blunt tipped parts articulate dorsally with the anterior margins of the scapulae.

In conclusion, based on the novel data on the pectoral elements in IVPP V 15001, it allows for the reassignment of specimen PIMUZ T 1559 to *M. fuyuanensis*, and thus underscores the widespread distribution of the species from the eastern to the western Tethyan provinces in the Middle Triassic.

Acknowledgements SNFS and TMS acknowledge the great hospitality and support of the IVPP during their research stay. Zheng F. and Geng B.-H. (IVPP) are thanked for observations on and their assistance with IVPP V 15001. V. Jaquier and H. Furrer (both Zurich) are thanked for discussions and C. Klug for access to the PIMUZ specimens under his care. Jiang D.-Y. (PKU) is warmly thanked for access to the PKU specimen of *Macrocnemus*. IVPP V 15001 was skillfully prepared by Ding Jinzhao (IVPP). We thank editor Zhou Shuang and the reviewers Wu Xiao-Chun and Liu Jun for their helpful and constructive comments. The Swiss National Science Foundation (grant no. 205321_162775), the Strategic Priority Research Program (B) of the Chinese Academy of Sciences (grants XDB26000000) and the National Natural Science Foundation of China (NSFC grants 41772006) supported this research.

中国中三叠世富源巨脰龙(主龙型小纲, 长颈龙科)的骨骼学再描述

Torsten M. SCHEYER¹ 王 维^{2,3,4} 李 淳^{3,4} Feiko MIEDEMA^{1,5}

Stephan N. F. SPIEKMAN¹

(1 瑞士苏黎世大学古生物研究所及博物馆 苏黎世 CH-8006)

(2 中国科学院地质与地球物理研究所, 岩石圈演化国家重点实验室 北京 100029)

(3 中国科学院古脊椎动物与古人类研究所, 中国科学院脊椎动物演化与人类起源重点实验室 北京 100044)

(4 中国科学院生物演化与环境卓越创新中心 北京 100044)

(5 德国斯图加特自然历史博物馆 斯图加特 D-70191)

摘要: 过去数十年里, 中国西南地区的中三叠统产出了越来越多的爬行动物化石。以海龙类、鱼龙类和鳍龙类为主的海生爬行动物, 广泛分布于整个特提斯洋周边。甚至有一些物种在这古海洋的东、西两侧, 即现在的中国和欧洲都有报道。最近发现的富源巨脰龙(*Macrocnemus fuyuanensis*)是较为罕见的陆生物种, 该种最初发现于云南中三叠统。瑞士南部的世界遗产地圣乔治山动物群中发现的一零散标本也曾被初步推断属于该物种(作为归入种: *Macrocnemus* aff. *M. fuyuanensis*)。由于最初对富源巨脰龙模式标本的解剖学记述有限, 这一归入仅基于肢骨比例而不是骨骼特征。本文对富源巨脰龙的模式标本进行了重新描述, 并与已知归入标本进行了比较。研究发现, 富源巨脰龙模式标本的肩带保存比从前报道的更加完整, 间锁骨形态可以被明确, 而这一结构在中国唯一归入标本中只是部分暴露, 但在欧洲归入标本中保存完好。在区别巨脰龙属的不同种时, 推测除了肢骨比例之外, 间锁骨的形态特征最为重要: 富源巨脰龙间锁骨的后突短且呈纺锤状, 间锁骨前缘有一对棒状的突起, 从前缘中间的V形凹槽处延伸而出, 以此可与巴氏巨脰龙(*Macrocnemus bassanii*)相区别。此外, 进一步详细研究了富源巨脰龙模式标本的颅骨解剖特征, 发现与巴氏巨脰龙完全相同。以往对巨脰龙的腭部知之甚少, 保存精美和精心修理的标本为了解该部形态特征增加了重要的信息。

关键词: 特提斯, 三叠纪, 拉丁期, 法郎组, 陆生爬行动物, 主龙型类, 长颈龙类

中图法分类号: Q915.864 **文献标识码:** A **文章编号:** 1000-3118(2020)03-0169-19

References

- Camp C L, 1945. *Prolacerta* and the protorosaurian reptiles. Part II. Am J Sci, 243: 84-101
- Fraser N, Furrer H, 2013. A new species of *Macrocnemus* from the Middle Triassic of the eastern Swiss Alps. Swiss J Geosci, 106: 199-206
- Huene F v, 1946. Die grossen Stämme der Tetrapoden in den geologischen Zeiten. Biologisch Zentralbl, 65: 268-275
- Jaquier V P, Fraser N C, Furrer H et al., 2017. Osteology of a new specimen of *Macrocnemus* aff. *M. fuyuanensis* (Archosauromorpha, Protorosauria) from the Middle Triassic of Europe: potential implications for species recognition and paleogeography of tanystropheid protorosaurs. Front Earth Sci, 5: 91, doi:10.3389/feart.2017.00091

- Jiang D Y, Rieppel O, Fraser N C et al., 2011. New information on the protorosaurian reptile *Macrocnemus fuyuanensis* Li et al., 2007, from the Middle/Upper Triassic of Yunnan, China. *J Vert Paleont*, 31: 1230–1237
- Kuhn-Schnyder E, 1962. Ein weiterer Schädel von *Macrocnemus bassanii* Nopcsa aus der anisischen Stufe der Trias des Monte San Giorgio (Kt. Tessin, Schweiz). *Paläontol Z*, 36(S1): 110–133
- Li C, Zhao L J, Wang L T, 2007. A new species of *Macrocnemus* (Reptilia: Protorosauria) from the Middle Triassic of southwestern China and its palaeogeographical implication. *Sci China Ser D: Earth Sci*, 50(11): 1601–1605
- Nopcsa F B, 1930. Notizen über *Macrocnemus bassanii* nov. gen. et spec. *Cbl Min*, 1930: 252–255
- Peyer B, 1937. Die Triasfauna der Tessiner Kalkalpen. XII. *Macrocnemus bassanii* Nopcsa. *Abh schweiz Paläontol Gesellsch*, 59: 1–140
- Pritchard A C, Turner A H, Nesbitt S J et al., 2015. Late Triassic tanystropheids (Reptilia, Archosauromorpha) from northern New Mexico (Petrified Forest Member, Chinle Formation) and the biogeography, functional morphology, and evolution of Tanystropheidae. *J Vert Paleont*, 35: e911186
- Rieppel O, 1989. The hind limb of *Macrocnemus bassanii* (Nopcsa) (Reptilia, Diapsida): development and functional anatomy. *J Vert Paleont*, 9: 373–387
- Rieppel O, Li C, Fraser N C, 2008. The skeletal anatomy of the Triassic protorosaur *Dinocephalosaurus orientalis* Li, from the Middle Triassic of Guizhou Province, southern China. *J Vert Paleont*, 28: 95–110
- Spiekman S N F, Scheyer T M, 2019. A taxonomic revision of the genus *Tanystropheus* (Archosauromorpha, Tanystropheidae). *Palaeontol Electron*, 22(3): 1–46
- Welman J, 1998. The taxonomy of the South African proterosuchids (Reptilia, Archosauromorpha). *J Vert Paleont*, 18: 340–347